Am J Cancer Res 2022;12(7):3034-3050
www.ajcr.us /ISSN:2156-6976/ajcr0142960

Original Article

The functions and prognostic values of chemokine and chemokine receptors in gastric cancer

Chenglong He[1], Liping He[2], Qiaowei Lu[1], Jianjun Xiao[1], Wenjing Dong[1]

[1]*Department of Oncology, Zhongshan City People's Hospital, Zhongshan 528400, Guangdong, China;*
[2]*Guangdong Provincial People's Hospital Zhuhai Hospital, Zhuhai 519040, Guangdong, China*

Received March 18, 2022; Accepted June 8, 2022; Epub July 15, 2022; Published July 30, 2022

Abstract: Chemokine and chemokine receptors (CCRs) play a significant role in tumor infiltration of immune cells, tumor angiogenesis and distant metastasis. In this study, we explored the importance of CCRs in gastric cancer (GC) by analyzing the datasets from TCGA database. First, we analyzed the characteristics of the CCRs mutations. Then, we screened the differentially expressed CCRs and performed GO functional annotation and KEGG pathway analyses to explore their potential biological functions. Using multivariate Cox regression analyses, we constructed a prediction model based on four-CCRs (CCL15, CCL21, CCR3 and ACKR3) signature, and we found that the risk score of the model was an independent prognostic factor of GC. Next, a nomogram was constructed to assess the prognosis of GC patients. GSEA indicated that the high-risk group was significantly enriched in immune response and immune system process. Moreover, GSVA was employed to investigate the up- and down-regulated signaling pathways in the high- and low-risk groups. The correlation between risk score and immune-cell infiltration indicated that the four-CCRs signature might play a pivotal role in GC immune microenvironment. In conclusion, we revealed the potential molecular mechanisms of CCRs in GC and constructed a prediction model which might guide personalized treatment and prognosis for GC patients.

Keywords: Chemokine, chemokine receptors, gastric cancer, prognosis, immune infiltrates

Introduction

Gastric cancer (GC) is the third leading cause of cancer deaths around the world [1, 2]. About two-third GC patients were diagnosed as advanced GC, and many patients will have local recurrence and distant metastasis even after receiving the radical resection [3]. The 5-year survival rate of advanced GC patients is only about 5%-20%, with 10 months of the overall survival (OS) [4, 5]. Although some biomarkers related to the tumorigenesis and prognosis of GC have been evaluated [6], the methods that could accurately predict the prognosis of GC patients remain limited. Therefore, it is an urgent need to develop predictive models for the improved prognosis and treatment of GC patients.

Chemokines are small, secreted chemoattractant molecules that can regulate immune and inflammatory response, cell migration, proliferation and survival, which play an important role in various biological and pathological processes including cancer [7]. So far, more than 50 chemokines and 20 chemokine receptors have been identified [8]. According to the primary structure of the peptide chain, chemokines are classified into 4 subfamilies: CC, CXC, XC, and CX3C. The typical chemokine receptors are also divided into four subfamilies based on their binding ligand specificity: CCR (CCR1-CCR11 and CXCR (CXCR1-CXCR6)) [9]. Recently, some atypical chemokine receptors (ACKRs), e.g., ACKR1/2/3/4, have also been identified [10]. Unlike the typical chemokine receptors, ACKRs cannot trigger the canonical G protein mediated signaling, but they can combine with typical cytokines and regulate the chemokine network [11].

Many studies have revealed that tumor and its microenvironment (TME) contain a complex chemokine network [12]. Chemokine and che-

mokine receptors (CCRs) may affect the degree of immunocyte infiltration and phenotype [13-15], angiogenesis [16, 17], tumor cell growth [18, 19], metastasis [20, 21], and survival [22], which, in turn, affect the patient's prognosis. For example, CC and CXC (e.g., CCL2, CCL5, CXCL1 and CXCL5) chemokines can recruit monocytes and neutrophils to the tumor microenvironment where monocytes and neutrophils can promote or inhibit tumor progression [13-15, 23]. CXCL12 and CCL2 have been found to promote angiogenesis in ovarian cancer [24, 25]. CCL28 can modulate MAPK/ERK pathway to promote breast cancer cell growth and metastasis [21]. ACKR3 promotes epithelial to mesenchymal transition (EMT) and tumor growth by mediating TGF-β1 function in lung cancer [26]. Indeed, some monoclonal antibodies and chemokine receptor inhibitors have already been used in the clinical practice for malignant tumor treatment. For example, CXCR4 antagonist (AMD3100) is used to treat relapsed or refractory acute myeloid leukemia (AML) [27]. CCL2 inhibitor (CNTO 888) is used to treat metastatic prostate cancer [28, 29], and anti-CCR4 monoclonal antibody (Mogamulizumab) is used to treat T-cell leukemia-lymphoma [30]. They have shown some therapeutic effects, and more clinical studies targeting CCRs are in progress. Nevertheless, although some CCRs (e.g., CCR5 and its ligand) were found differentially expressed in GC, and their expression is associated with a poor prognosis [31], the role of most CCRs in GC progression has not been reported. Therefore, our current studies aimed to identify the potential biological function and signature of CCRs to improve prognostic evaluation of GC. By multivariate Cox regression analysis, a novel four-CCRs (CCL15, CCL21, CCR3 and ACKR3) signature was constructed.

Methods

Data extraction and data processing

Genetic mutation data, transcriptome data, and clinical data of GC samples were obtained from the TCGA database (https://portal.gdc.cancer.gov/). Mutation data were visualized using the "maftools" package in R (4.1.0).

CCRs expression in GC

Differentially expressed CCRs between tumor and normal samples were analyzed and visualized using the "limma" and "pheatmap" package in R (4.1.0). The threshold of adjusted false discovery rate was <0.05 with |log2 (fold change)| >1. *P*-values less than 0.05 were considered statistically significant. Spearman correlation analysis was used to evaluate the correlation of CCRs expressions. $P<0.05$ was selected as statistically significant.

Enrichment analysis of CCRs

To explore the functional mechanisms of CCRs in GC, we performed GO functional annotation and KEGG pathway enrichment analysis in R (4.1.0) by employing the packages "GO plot", "Cluster Profiler", "ggplot2", "DOSE" and their dependency packages. The enriched GO terms, KEGG pathways and PPI network were further annotated and visualized by Metascape [32].

Establishment and verification of the prognostic model

First, Kaplan-Meier analysis was performed to screen CCRs with prognostic values. Then, multivariate Cox regression was performed to construct CCRs-related prognostic signature and calculate the risk score of each patient. Risk scores were generated based on the expression of genes multiplied by a linear combination of regression coefficients obtained from the multivariate Cox regression analysis ($P<0.01$ was considered statistically significant). The formula used in CCRs model was: risk score= $\sum_{i=1}^{n} vi \times ci$. (*n*: the quantity of independent indicators, *vi*: the expression quantity of gene, *ci*: the regression coefficient of gene i in multivariate Cox regression analysis). All GC patients were divided into two groups by the median risk score. We plotted K-M survival curve which was tested by log rank to portion statistical significance for evaluating the discrepancy of OS between the two groups. Besides, we plotted ROC curves by the "survival ROC" package in R (4.1.0) to verify the accuracy of this model. Principal component analysis (PCA) was conducted based on the "prcomp" package in R (4.1.0). To verify whether the risk score could be used as an independent prognostic factor for GC, univariate and multivariate analyses were performed by adopting the Cox regression method. A nomogram was built to investigate the probability of prognosis in GC patients.

Immunohistochemistry

The immunohistochemistry images for the expression of ACKR3, CCR3, and CCL21 in GC tissues and normal tissues were downloaded from the Human Protein Atlas (https://www.proteinatlas.org/).

RNA extraction and real-time PCR

Total RNA was extracted by Trizol reagent (Invitrogen, Carlsbad, CA, United States) according to the manufacturer's protocol. Subsequently, the extracted RNA was reverse transcribed using PrimeScript RT reagent Kit with gDNA Eraser (Takara, Japan). The cDNAs were subjected to SYBR Green-based real-time PCR analysis. The primers used in real-time PCR assays were listed in Table S1.

Correlation between the risk score and immune cell infiltration

The Tumor Immune Estimation Resource (TIMER) database [33] was employed to analyze the correlation between the risk score and tumor-infiltrating immune cells (B cells, $CD4^+$ T cells, $CD8^+$ T cells, neutrophils, macrophages and dendritic cells). The abundance of the six immune infiltrates was estimated by the TIMER algorithm in R (4.1.0).

GSEA and GSVA functional annotation

We performed GSEA by using the software Gene Set Enrichment Analysis (GSEA) v4.0.3. The Gene Set Variation Analysis (GSVA) analysis was performed using "GSVA" package in R (4.1.0) using C2 gene sets (KEGG) from MSigDB (http://www.gsea-msigdb.org/gsea/index.jsp).

Statistical analysis

All statistical analyses were performed by R (version 4.1.0). $P<0.05$ was considered statistically significant except for special notes.

Results

Ccrs mutation analysis in GC samples

The incidence of copy number variations and somatic mutations of 63 CCRs in GC samples were summarized in **Figure 1**. Among the 132 samples we examined, 82 samples contained mutations of CCRs, with the frequency of 62.88%. The top 30 frequently mutated genes were shown in the waterfall plot, and the top 10 commonly mutated genes were CX3CL1, XCR1, CCR1, CXCR1, CXCR2, CCR3, CCR5, CCR7, CXCL16 and ACKR4. Among them, CX3CL1 and XCR1 were the highest mutated genes with more than 5% mutation rates (**Figure 1A**). Besides, the three most common mutation types were missense mutation, followed by frameshift deletions and frameshift insertions (Figure S1A). In addition, we found that there were some co-occurring mutations (e.g., CXCR6/CCR9, CCL1/CXCR1, ACKR1/CCR7 and ACKR4/CXCL16) of CCRs in GC samples (**Figure 1B**).

Expression of CCRs between GC and normal tissues

Since genetic variations could be the prominent factor influencing the expression of CCRs, we further compared the differential expression of 63 CCRs between cancer and normal tissues (**Figure 2A**). We found that 41 CCRs were differentially expressed between GC and normal tissues, and the expression of the majority of these genes were up regulated in GC (**Figure 2B**). The most differentially expressed 24 CCRs ($P<0.01$, $|logFC| >1$) were shown in (**Table 1**). Moreover, spearman correlation analysis was used to investigate the correlation between the 63 CCRs and GC, and we observed both positive and negative correlations between the expression of these genes and GC (Figure S2). The genes with the strongest positive correlation were CXCL10 and CXCL11 ($R=0.92$), and the genes with strongest negative correlation were CXCL16 and CCL14 ($R=-0.27$).

Functional annotation of the significant CCRs

To explore the biological functions and potential mechanisms of the CCRs, GO and KEGG pathway enrichment analyses were performed for the top 24 CCRs (**Table 1**) with the significant expression change in GC. The GO analysis showed that these CCRs were mostly enriched in chemokine-mediated signaling pathways (BP), external side of plasma membrane (CC), and the chemokine activities (MF) (**Figure 3A**). From the KEGG pathway analysis, we found that these differentially expressed CCRs were mainly associated with viral protein interaction

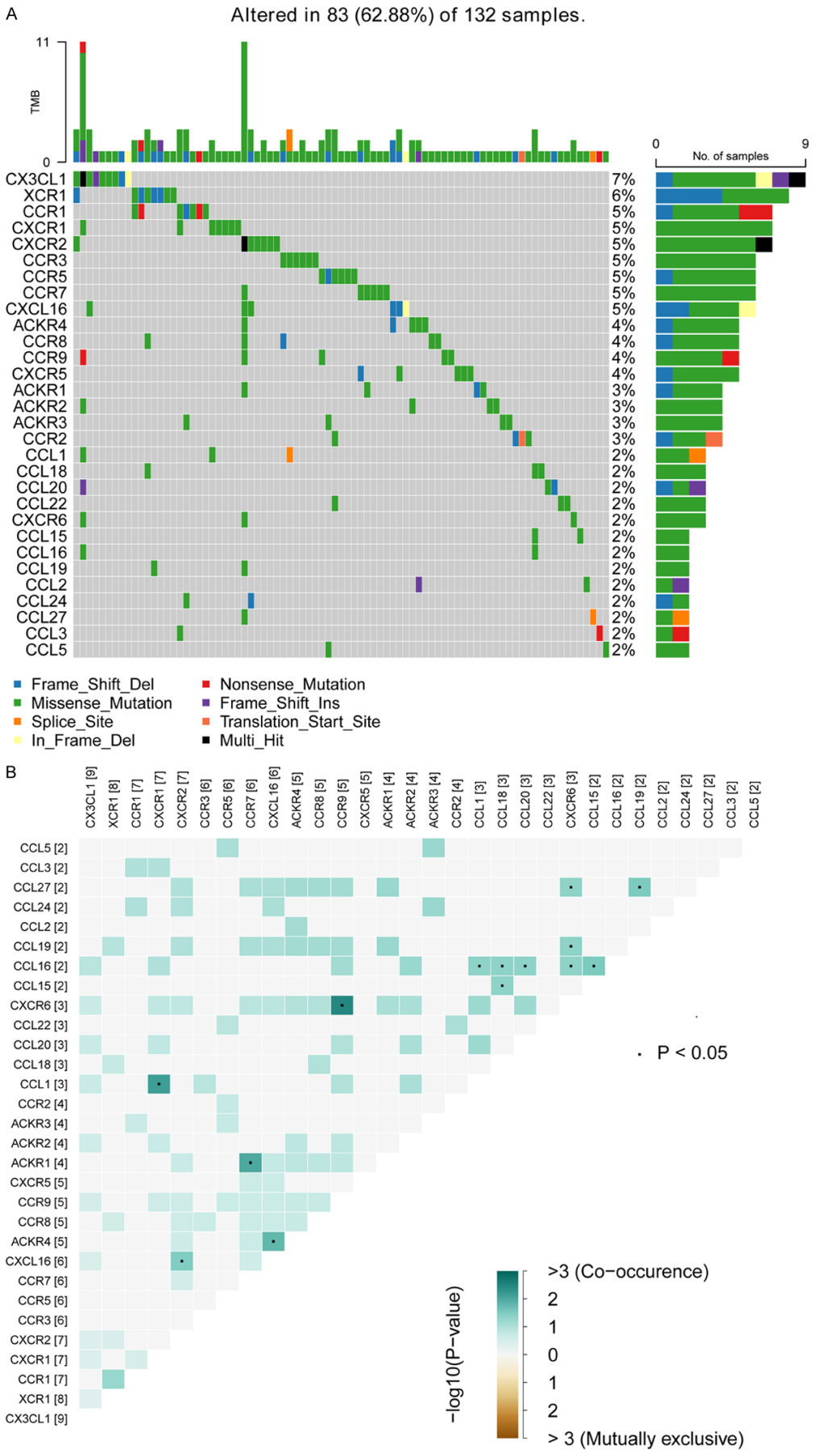
A
Altered in 83 (62.88%) of 132 samples.
TMB
11
0
No. of samples
0
9
CX3CL1 7%
XCR1 6%
CCR1 5%
CXCR1 5%
CXCR2 5%
CCR3 5%
CCR5 5%
CCR7 5%
CXCL16 5%
ACKR4 4%
CCR8 4%
CCR9 4%
CXCR5 4%
ACKR1 3%
ACKR2 3%
ACKR3 3%
CCR2 3%
CCL1 2%
CCL18 2%
CCL20 2%
CCL22 2%
CXCR6 2%
CCL15 2%
CCL16 2%
CCL19 2%
CCL2 2%
CCL24 2%
CCL27 2%
CCL3 2%
CCL5 2%
Frame_Shift_Del
Missense_Mutation
Splice_Site
In_Frame_Del
Nonsense_Mutation
Frame_Shift_Ins
Translation_Start_Site
Multi_Hit
B
CX3CL1 [9]
XCR1 [8]
CCR1 [7]
CXCR1 [7]
CXCR2 [7]
CCR3 [6]
CCR5 [6]
CCR7 [6]
CXCL16 [6]
ACKR4 [5]
CCR8 [5]
CCR9 [5]
CXCR5 [5]
ACKR1 [4]
ACKR2 [4]
ACKR3 [4]
CCR2 [4]
CCL1 [3]
CCL18 [3]
CCL20 [3]
CCL22 [3]
CXCR6 [3]
CCL15 [2]
CCL16 [2]
CCL19 [2]
CCL2 [2]
CCL24 [2]
CCL27 [2]
CCL3 [2]
CCL5 [2]
P < 0.05
−log10(P−value)
>3 (Co−occurence)
2
1
0
1
2
> 3 (Mutually exclusive)

Figure 1. Mutation profile analysis of CCRs by using the TCGA datasets. A. Oncoplot displaying the somatic landscape of the top 30 CCRs in GC samples from TCGA database. B. The co-occurring mutations and the mutual exclusivity analysis of the top 30 CCRs. Co-occurrence, green; Exclusion, brown.

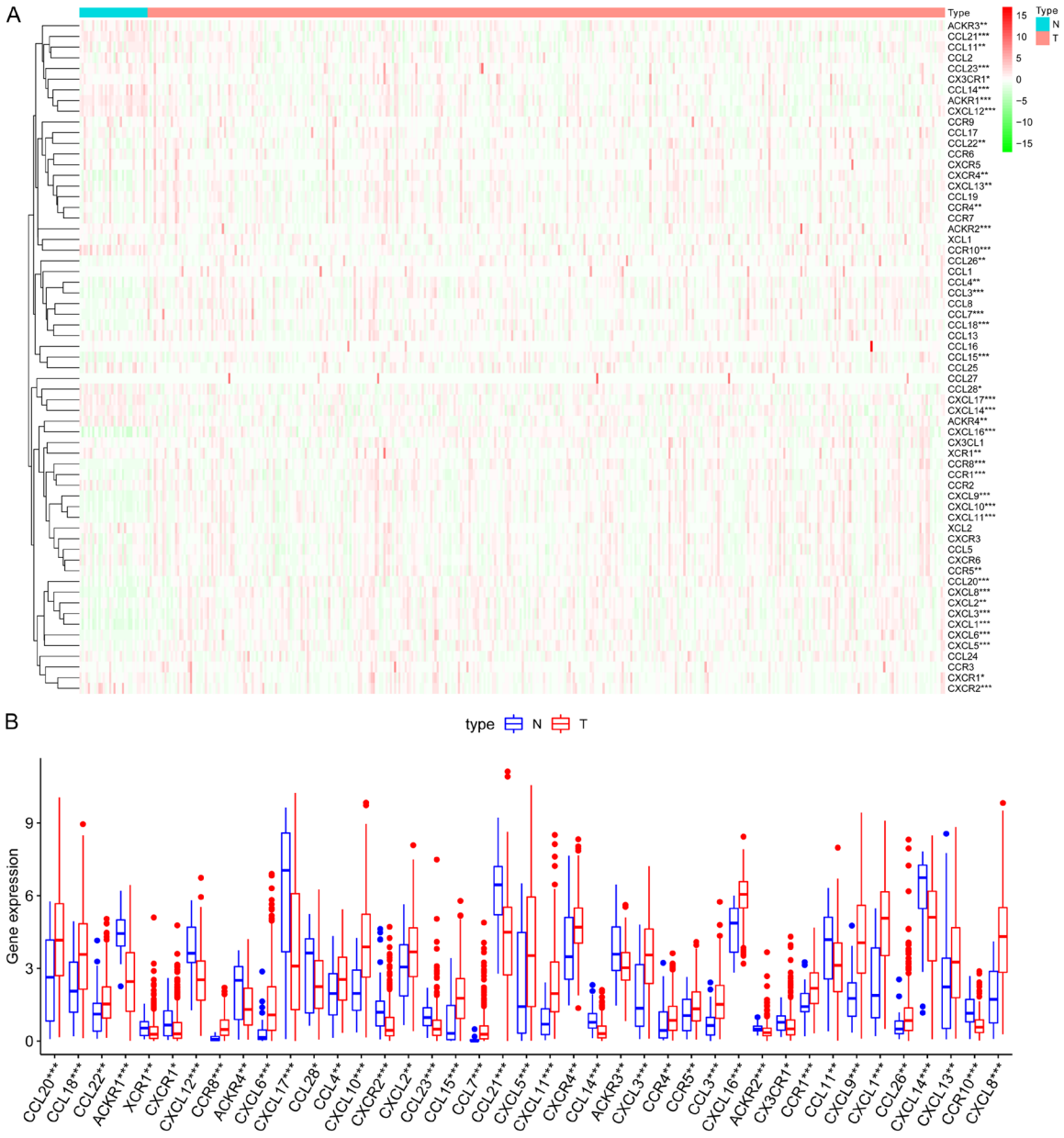

Figure 2. Expression analysis of CCRs. A. The expression levels of CCRs in the TCGA datasets. Red indicates up-regulated genes; green indicates down-regulated genes. B. Boxplot displaying the differentially expressed CCRs in GC. Blue, normal. Red, tumor. Not significant (ns), P<0.05 (*), P<0.01 (**), and P<0.001 (***).

with cytokine and cytokine receptor, chemokine signaling pathway and cytokine-cytokine receptor interaction (**Figure 3B**). Annotation of GO, KEGG pathways enrichment analysis and PPI network of these top 24 CCRs were also performed using "Metascape" website (**Figure 3C**; Figure S3). As shown in **Figure 3D**, 16 hub genes were identified in the protein - protein interaction network.

Construction of a prognostic risk model

To analyze the relationship between the expression of CCRs and the prognosis of GC, univari-

Table 1. Expression of top 24 CCRs

gene	normalMean	tumorMean	logFC	*P*-value
CXCR2	3.77726971	1.112872577	-1.763055385	0.000365247
CXCL17	225.559568	73.02803964	-1.626986074	6.88E-05
ACKR1	25.204637	9.336958332	-1.432664629	4.25E-11
CCL21	118.318518	47.5927657	-1.313861685	1.02E-08
CCL14	0.98009266	0.411905058	-1.250606306	1.42E-07
CXCL12	17.373577	7.517509883	-1.208568054	1.03E-07
CCR10	1.56625757	0.688337184	-1.186134135	3.39E-06
CCR1	2.33214037	4.821027975	1.047686176	2.85E-05
CCL15	1.70143162	3.992240417	1.230449429	4.48E-06
CXCL16	28.7594958	72.58288985	1.335591117	3.20E-11
CXCL3	5.89865494	18.03349774	1.612221323	8.26E-07
CCL3	0.80032764	3.439417526	2.103501615	1.09E-09
CCL20	10.9999174	52.1466439	2.245081718	6.27E-05
CCL18	6.14431732	29.29875169	2.253514568	3.47E-05
CCL26	0.68780889	3.814495172	2.47141247	0.001664114
CXCL5	12.2286623	72.64480995	2.57059314	0.000747777
CCR8	0.08748828	0.585523355	2.742565112	6.26E-13
CXCL1	8.4535364	63.02696675	2.898342332	5.31E-11
CXCL6	0.50611615	4.143685123	3.033373974	3.59E-09
CXCL10	4.4314276	41.13843483	3.214643458	6.28E-10
CXCL11	1.00251453	10.61476438	3.404377294	5.41E-10
CXCL9	4.16285404	45.28027036	3.443237691	4.08E-11
CXCL8	4.26019156	49.03128271	3.524712298	4.08E-11
CCL7	0.03366889	0.777061946	4.528541442	7.91E-13

ate Cox regression analysis was performed for the 63 CCRs. The results indicated that 7 CCRs were significantly correlated with the survival of GC patients (**Figure 4A**). In addition, multivariate Cox regression analysis was performed to construct a prognostic risk model using four genes (CCL15, CCL21, CCR3 and ACKR3) and to calculate the risk score for each patient (**Table 2**). Based on the median risk score, 368 GC patients were divided into high-risk group (n=184) and low-risk group (n=184). The survival overview and gene expression heatmaps of these two groups were presented in **Figure 4B**. By analyzing the expression data of all genes (**Figure 4C**) and the risk-related genes (**Figure 4D**), principal component analysis (PCA) was performed, and we found that our risk score could accurately distinguish the high- and low-risk groups. Kaplan-Meier analysis indicated that, compared with the low-risk group, the prognosis of the high-risk group was significantly worse (P<0.01) (**Figure 4E**). The AUC of the ROC curve was 0.825, suggesting our model had a good performance in predicting the prognosis of GC patients with high sensitivity and specificity (**Figure 4F**).

Validation and application of the prognostic risk model

To evaluate the independent prognostic ability of our prognostic model, univariate (**Figure 5A**; **Table 3**) and multivariate (**Figure 5B**; **Table 4**) Cox regression analyses were performed to explore the relationship between clinicopathological characteristics and patient prognosis. The results showed that the risk score could be used as an independent predictor of the prognosis of GC patients (P<0.001). To facilitate the clinical use of this model to obtain reliable prognostic information of each patient, we constructed a nomogram that could predict the 1-, 2- and 3-year OS probability of GC patients (**Figure 5C**).

Protein and mRNA expression of CCL15, CCL21, CCR3 and ACKR3

To reveal the protein expression profile of CCL15, CCL21, CCR3 and ACKR3 in normal tis-

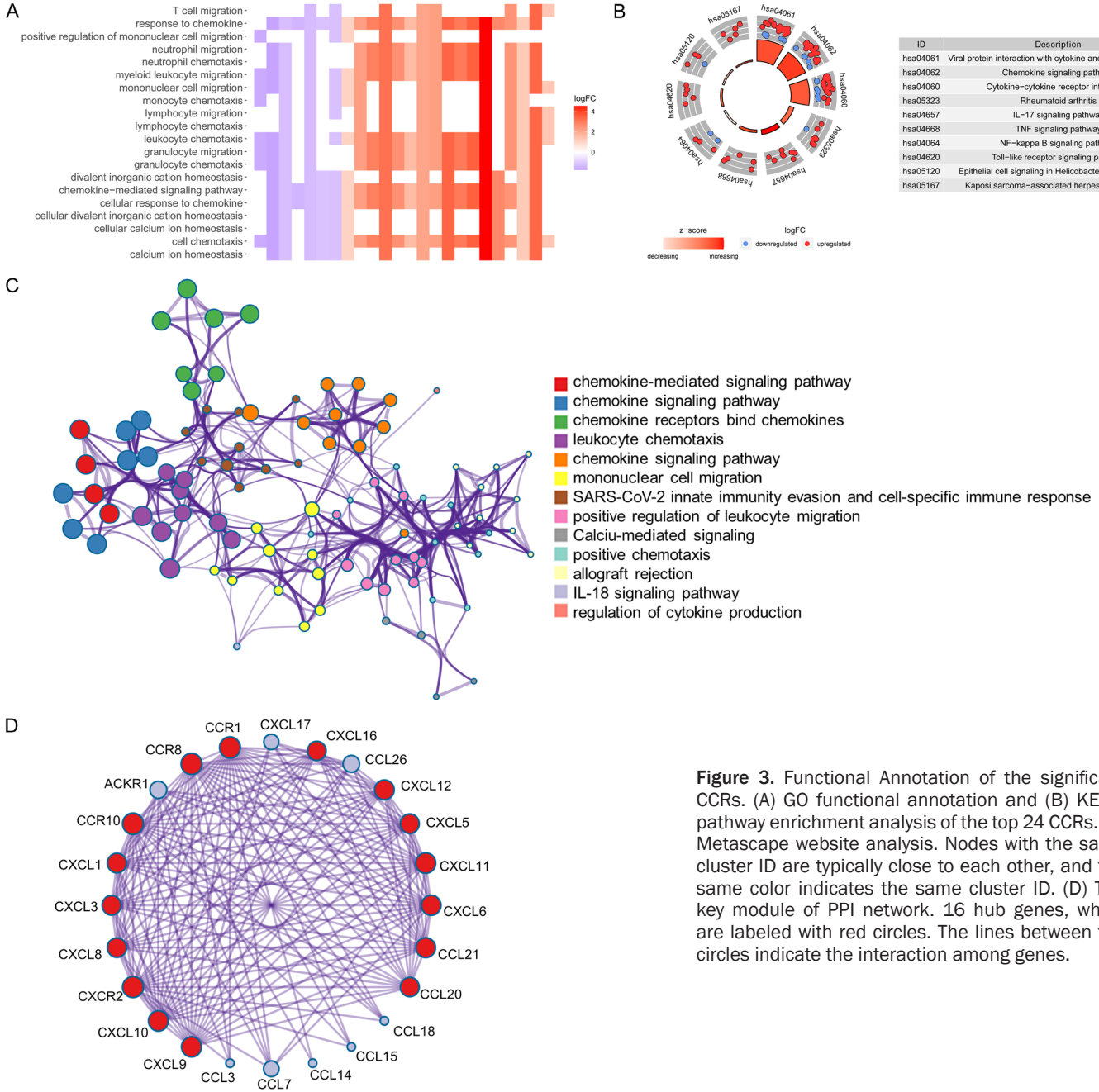

ID	Description
hsa04061	Viral protein interaction with cytokine and cytokine receptor
hsa04062	Chemokine signaling pathway
hsa04060	Cytokine−cytokine receptor interaction
hsa05323	Rheumatoid arthritis
hsa04657	IL−17 signaling pathway
hsa04668	TNF signaling pathway
hsa04064	NF−kappa B signaling pathway
hsa04620	Toll−like receptor signaling pathway
hsa05120	Epithelial cell signaling in Helicobacter pylori infection
hsa05167	Kaposi sarcoma−associated herpesvirus infection

Figure 3. Functional Annotation of the significant CCRs. (A) GO functional annotation and (B) KEGG pathway enrichment analysis of the top 24 CCRs. (C) Metascape website analysis. Nodes with the same cluster ID are typically close to each other, and the same color indicates the same cluster ID. (D) The key module of PPI network. 16 hub genes, which are labeled with red circles. The lines between the circles indicate the interaction among genes.

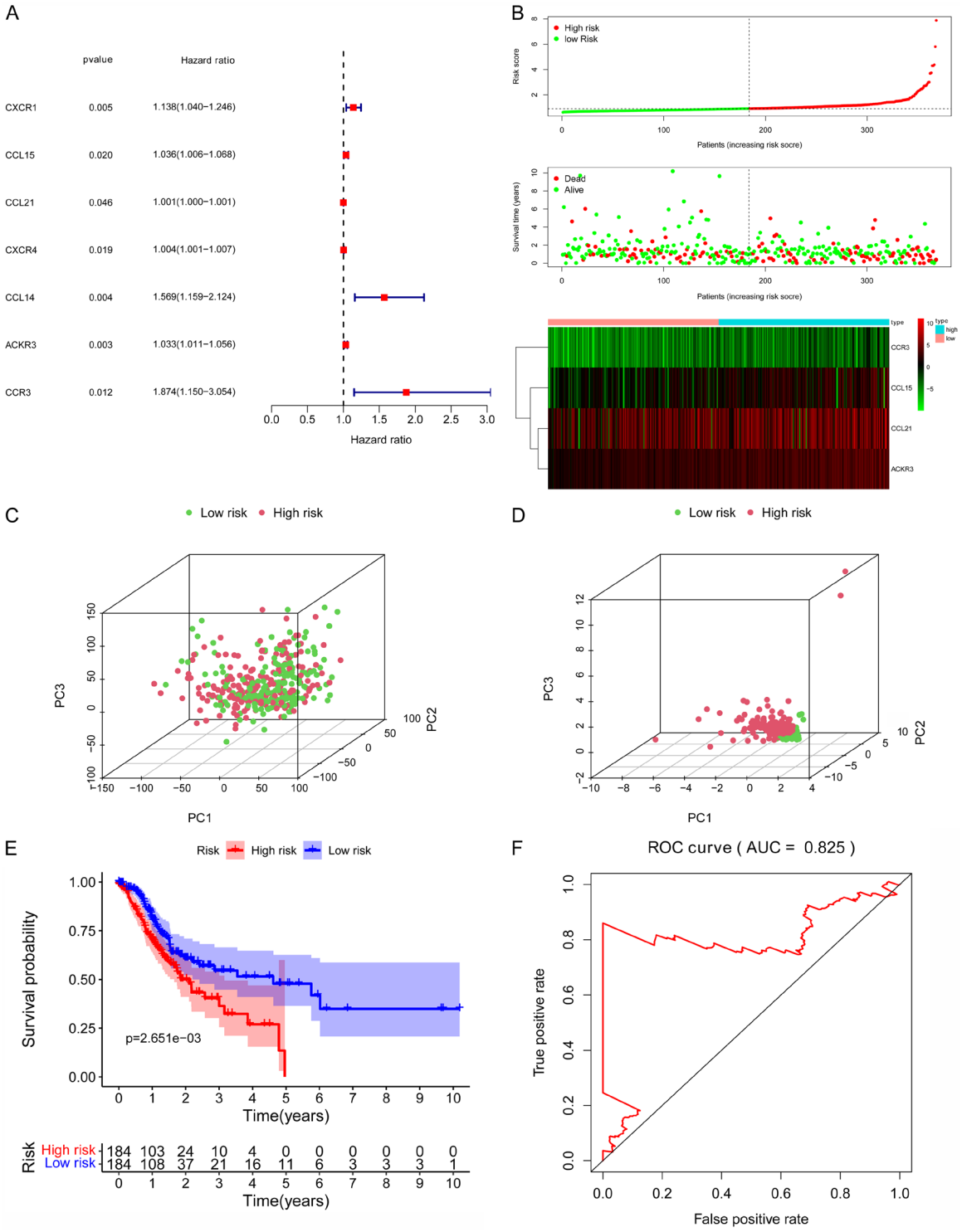

Figure 4. Prognostic value of CCRs in GC patients. (A) Univariate Cox regression analysis between CCRs expression and OS. (B) The distribution of prognostic signature-based risk scores. Principal component analysis between low-risk and high-risk groups for all genes (C) and for risk genes (D). (E) Kaplan-Meier survival curve for the OS of GC patients. The red line represents the high-risk group, and the blue line represents the low-risk group. (F) AUC of time-dependent ROC curve analysis for evaluating the prognostic performance of the risk score for 5-year OS.

sues and GC tissues, we extracted the relevant data from the Human Protein Atlas (HPA) website. As shown in **Figure 6A-F**, compared with normal tissue, ACKR3 was highly expressed,

Table 2. Four CCRs that constitute the CCRs-related prognostic model

Gene symbol	Coef	HR	HR.95L	HR.95H	*P*-value
CCL15	0.03720978	1.03791073	1.00674268	1.070043714	0.016759
CCL21	0.00077528	1.00077558	1.000095965	1.00145566	0.025298
ACKR3	0.03137368	1.03187102	1.009468142	1.054771079	0.005088
CCR3	0.65784562	1.93062854	1.17316883	3.177144213	0.009644

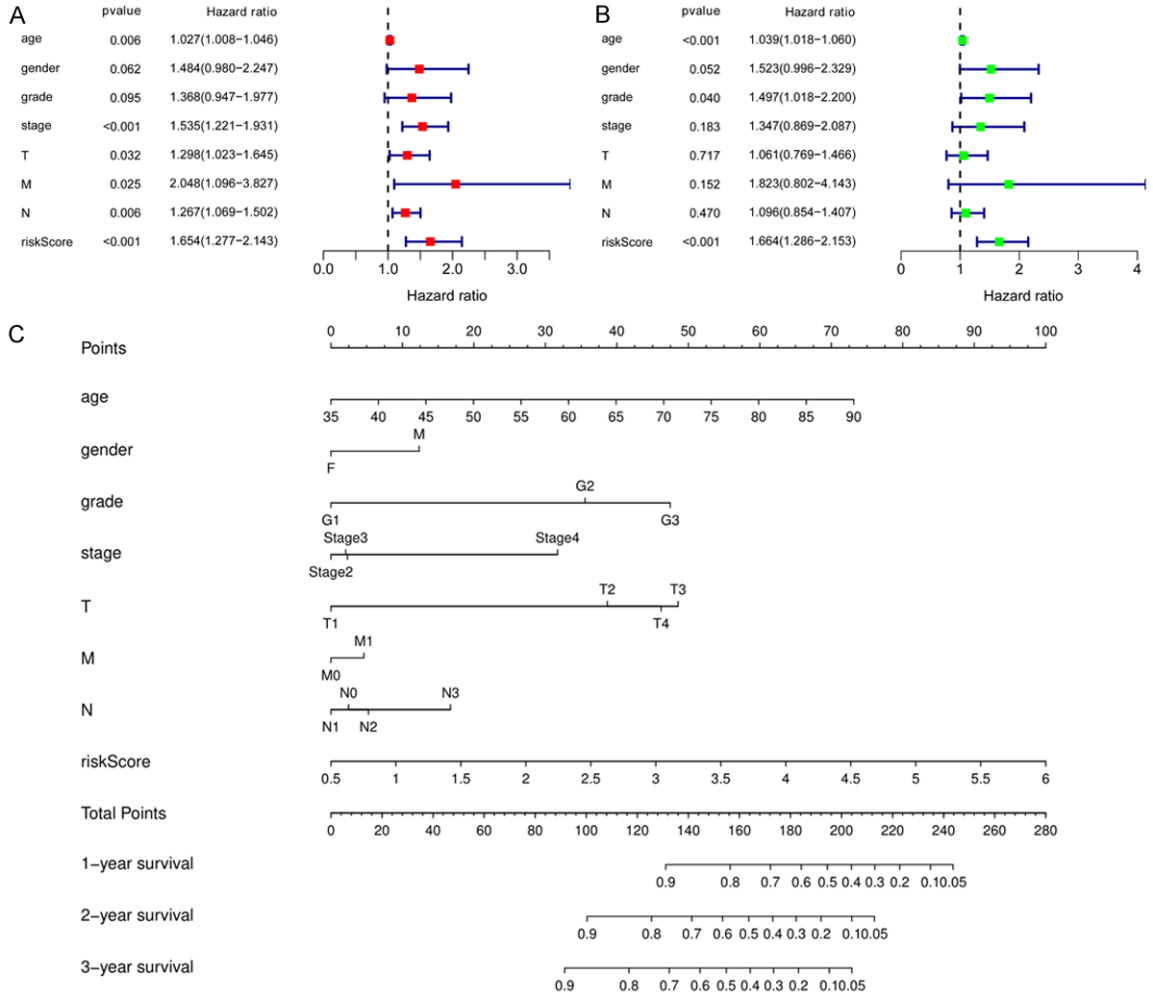

Figure 5. Validation and application of the prognostic risk model. A. Univariate Cox regression analysis. B. Multivariate Cox regression analysis. C. The nomogram for estimating the 1-, 2-, and 3-year overall survival of GC patients.

whereas the expression of CCR3 was lower in GC tissues. The expression of CCL21 was not detected in both normal and GC tissues, possibly due to its low expression level. The protein expression data of CCL15 was inaccessible in HPA database; hence, CCL15 expression was not presented in this study. We also verified the mRNA expression of the four genes using our own clinical samples (paired gastric cancer tissues, n=22). The results showed that CCL15, CCL21, CCR3, and ACKR3 were expressed differentially between normal and tumor tissues (**Figure 6G-J**).

The risk score was related to immunocyte infiltration

As mentioned above, CCRs were closely related to inflammatory response and tumor immunity. To explore whether the risk score was related to

Table 3. Univariate analyses of overall survival of GC patients by using TCGA datasets

Variables	HR	HR.95L	HR.95H	*P*-value
age	1.026965748	1.007829689	1.046465151	0.00556017
gender	1.483828302	0.979779065	2.247186647	0.062392212
grade	1.367875492	0.946580494	1.976676441	0.095375967
stage	1.535478376	1.221185829	1.930659353	0.000242497
T	1.297541887	1.023344886	1.645207762	0.031516711
M	2.048306027	1.096196896	3.827375896	0.024581693
N	1.267206892	1.068895108	1.5023114	0.006386528
riskScore	1.654379281	1.277259284	2.142846671	0.00013678

Table 4. Multivariate analyses of overall survival of GC patients by using TCGA datasets

Variables	HR	HR.95L	HR.95H	*P*-value
age	1.038699482	1.017970559	1.059850508	0.000222768
gender	1.523418052	0.996272439	2.329485862	0.052048908
grade	1.496553445	1.018153473	2.199739307	0.040217331
stage	1.346751999	0.869066971	2.086997905	0.182848275
T	1.061399022	0.768680251	1.465587131	0.717388532
M	1.822690208	0.80192462	4.142782887	0.151850095
N	1.096270464	0.854173045	1.406985312	0.470335302
riskScore	1.664082404	1.286237132	2.152923577	0.000106385

immune cell infiltration in GC, correlation analysis was carried out by using the TIMER Database. We found that the risk score was positively correlated with the infiltration of $CD4^+$ T cells, $CD8^+$ T cells, neutrophils, macrophages and dendritic cells (P<0.001) (**Figure 7A-E**), except for B cells (**Figure 7F**).

Functional enrichment analysis for different risk groups

GSEA was used to analyze the enrichment of high- and low-risk groups in two immune related gene sets. The results indicated that the high-risk group with poor survival was significantly enriched in these two immune related gene sets that included immune response and the process of immune system, while the low-risk group did not show such significant enrichment (**Figure 8A**). GSVA results indicated that, compared with the low-risk group, many metabolic pathways in the high-risk group were up-regulated or down regulated (**Figure 8B**, **8C**). These metabolic pathways included cytokine and cytokine receptor interaction, cell adhesion molecules (CAMs) and RNA degradation. The dysregulation of these pathways may be one of the factors affecting the prognosis of GC.

Discussion

Tumor immune microenvironment plays a very important role in anti-tumor activity [34, 35]. CCRs can affect the state of tumor immune microenvironment by regulating inflammatory response and immune cell infiltration [12, 36-38]. GC is a solid tumor which consists of stromal cells, e.g., endothelial cells and fibroblasts, and is infiltrated by various immune cells, e.g., $CD4^+$ T cells, $CD8^+$ T cells, neutrophils, macrophages, and dendritic cells. All these cells are involved in chemokine production [39]. Although some CCRs, e.g., CCR5 and its ligand, have been found differentially expressed in GC, and their expression is associated with aggressive tumor behavior and a poor prognosis [31], the role of most CCRs in GC progression has not been reported. Therefore, a comprehensive analysis and the molecular characterization of CCRs in GC will advance our understanding of the antitumor immune response and prognosis of GC.

In our current studies, we first systematically analyzed the mutation frequency and CNV alteration of CCRs by using the information from TCGA database. We found that the expression of most CCRs was dysregulated in GC.

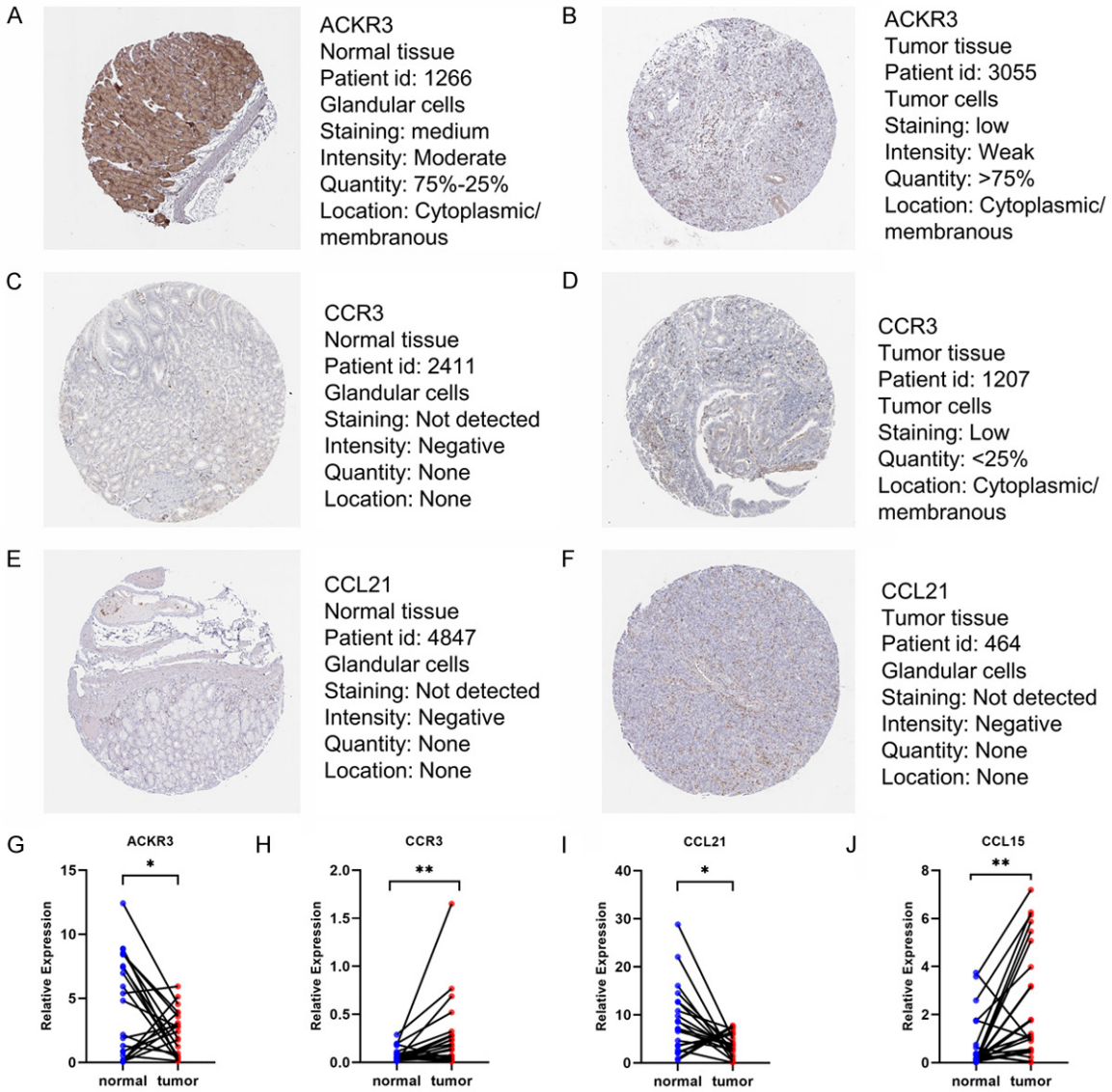

Figure 6. Immunohistochemical and qPCR analysis of ACKR3, CCR3, and CCL21. The expression of ACKR3 was higher in GC tissues than in normal tissues (A, B). The expression of CCR3 was lower in GC tissues than in normal tissues (C, D). The expression of CCL21 was not detected in both GC tissues and normal tissues (E, F). All results were obtained from HPA database. (G-J) mRNA relative expression of genes in the risk model by the method of qPCR.

Next, we selected the top 24 CCRs that exhibited significantly differential expression between normal and GC tissue for further investigation of their potential mechanisms and biological functions. As expected, these CCRs were significantly enriched in chemokine related gene sets and signaling pathways such as chemokine-mediated signaling pathway (BP), external side of plasma membrane (CC), chemokine activity (MF), viral protein interaction with cytokine (KEGG) and NF-kappa-B signaling pathway (KEGG). Consistent with our findings, it has recently been reported that the therapeutic concentration of 3,3'-Diindolylmethane (DIM) can upregulate the expression level of chemokines such as CCL-2 and activate NF-kappa-B signaling pathway in gastric cancer-derived mesenchymal stem cells, thus promoting the progression of GC [40]. In addition, we also conducted PPI analysis and found 16 hub genes that might play a key role in regulating the chemotaxis related molecular networks in GC.

Through multivariate Cox regression analyses, four CCRs (CCL15, CCL21, CCR3 and ACKR3)

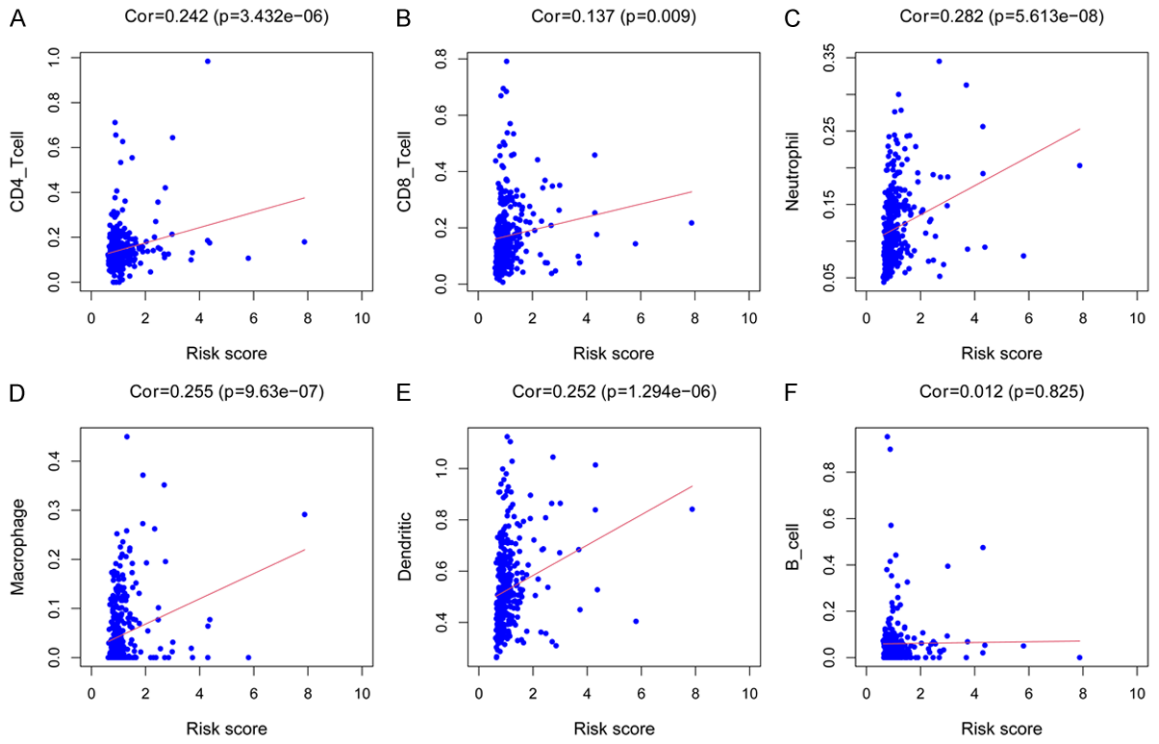

Figure 7. The correlation between risk scores and immune cell infiltrating. Neutrophils (A), $CD4^+$ T cells (B), $CD8^+$ T cells (C), dendritic cells (D), macrophages (E), and B cells (F) are revealed by scatter diagrams. The correlation is shown by Pearson correlation coefficient.

were identified to be significantly correlated with the OS of GC patients. Recently, there are studies showing the inflammatory response and pro-tumor or anti-tumor effect of these CCRs. For example, CCL15, acting mainly via CC chemokine receptor CCR1 [41], also binds to CCR3 [42] and can recruit immune cells, e.g., T-cells, monocytes, eosinophils, and neutrophils, to tumor microenvironment [42, 43] to induce tumor angiogenesis [44]. It has also been reported that CCL15 is highly expressed in digestive tract and liver tissues and plays an important role in maintaining the balance of immune response in these organs. In tumor, it is found that the accumulation of $CCR1^+$ tumor-associated neutrophils through CCL15-CCR1 axis can promote lung metastasis of colorectal cancer [45]. Moreover, CCL15 produced by the renal cell carcinoma cells that migrate to the bone has been shown to display a significant effect on osteoclastogenesis, and can promote the bone metastasis of tumor [46, 47]. CCL21, as the ligand for CCR7, can activate T cells, preferentially naive T cells [48, 49]. High expression of CCL21 in tumor can increase anti-tumor immune cell infiltration and prolong the survival of cancer patients [50, 51]. However, once the tumor immune microenvironment has been completely dysregulated, CCL21 may play an opposite role [52, 53] as CCL21 may recruit Treg into the tumor microenvironment, which results in tumor immune evasion. ACKR3 is the receptor for CXCL12 and CXCL11. Recent studies have shown that ACKR3 can promote tumor cell growth and metastasis [54, 55] through modulating the mTOR pathway [56]. Increased expression of ACKR3 is a significant prognostic factor for the poor prognosis of patients with aggressive prostate carcinoma [57] and renal carcinoma [58]. Based on the four CCRs (CCL15, CCL21, CCR3 and ACKR3) described above, we established a four-CCRs signature-associated risk model, and our results suggested that the risk score was an independent prognostic predictor for GC patients. Importantly, our GSVA results revealed some signaling pathways that were significantly different between high- and low-risk groups, such as cytokine and cytokine receptor interaction, cell adhesion molecules (CAMs) and RNA degradation. The abnormalities of these pathways may be the cause for the

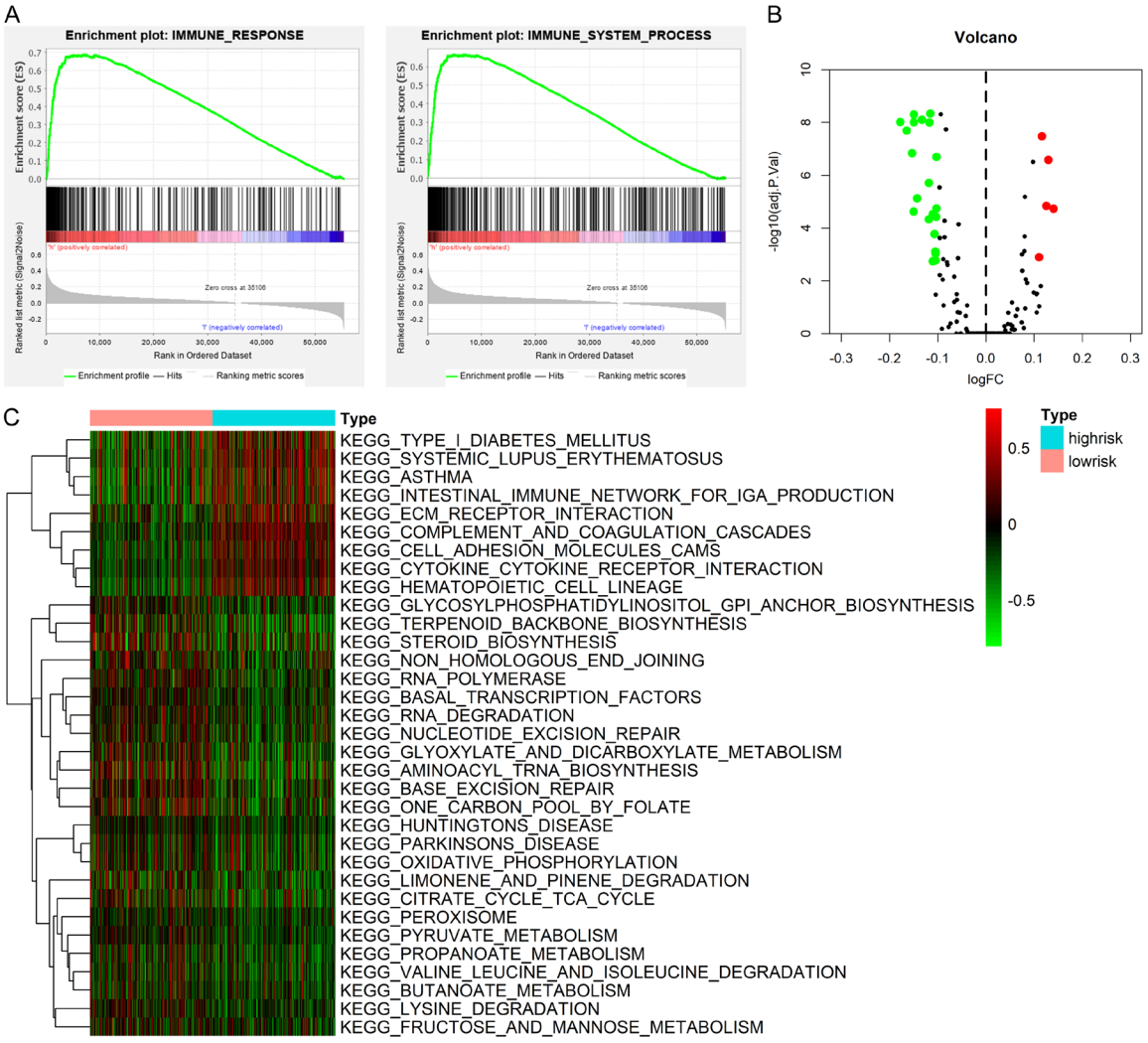

Figure 8. Differential signaling pathway enrichment in different risk groups. (A) gene sets of immune response and the process of Immune system in high-risk and low-risk groups analyzed by GSEA. (B, C) GSVA enrichment analysis showing the up and down regulated signaling pathways in different risk groups. Volcano plot (B), and Heatmap of differential expression in KEGG pathway (C). Red represents up regulated pathways, and green represents down regulated pathways.

difference in prognosis between high-risk and low-risk patients.

We further performed GSEA to determine the difference in immune responses between the high- and low-risk groups. Our results showed that the high-risk group was significantly enriched in two immune related gene sets including immune response and the process of immune system, while low-risk group showed no significant enrichment. This is in consistence with the fact that immune response plays an important role in anticancer immunity and is closely related to the prognosis of various human malignant tumors [59]. Tumor immune response involves many immune cells, and the role of immune cells is very complex and diverse. For example, neutrophils can promote the metastasis of tumor cells to distant organs by interacting with circulating tumor cells [60], and macrophages can promote EMT process to enhance tumor cells migration and invasion [61]. To understand the correlation between the risk score of our model and immune-cell infiltration, we conducted a correlation analysis based on the TIMER database. Our results indicated that the infiltration of $CD4^+$ T cells, $CD8^+$ T cells, neutrophils, macrophages and dendritic cells was positively associated with the risk score, suggesting that a

high infiltration level of these immune cells might increase the mortality risk of GC patients. However, in contrary to our results, high level of $CD4^+$ and $CD8^+$ cells infiltration in tumor has been reported as a good prognostic factor. We speculated that this contradiction was caused by the other functions of CCL21; the high expression of CCL21 might recruit Treg and lead to tumor immune escape.

Our research constructed a four-CCRs (CCL15, CCL21, CCR3 and ACKR3) signature prognostic risk model and provided new insights into the GC immune microenvironment. However, there are some limitations in this study. Since this was a retrospective study, the results need to be further validated by large-scale prospective studies. Besides, the predictive power of this model in GC requires further testing for better prognostic stratification and treatment management. Moreover, the biological functions of these four CCRs need further experimental verification.

Conclusion

Through a series of comprehensive analyses, we identified the potential biological function and prognostic value of CCRs in GC. We further constructed a novel prognosis model for GC patients. We found that the risk score of this model could reflect the immune microenvironment status of GC patients. The current studies shed some light on our understanding of CCRs in GC and provide novel potential prognostic and therapeutic biomarkers.

Acknowledgements

This study was funded by Science and Technology Projects Funding of Zhongshan Science and Technology Bureau (2018B1031).

Disclosure of conflict of interest

None.

Abbreviations

TCGA, The Cancer Genome Atlas; CCRs, Chemokine and chemokine receptors; GC, gastric cancer; GO, Gene Ontology; CC, Cellular Component; MF, Molecular Function; BP, Biological Process; ROC, receiver operating characteristic; OS, overall survival; GSVA, Gene Set Variation Analysis; AUC, area under the curve; KEGG, Kyoto Encyclopedia of Genes and Genomes; GSEA, Gene Set Enrichment Analysis.

Address correspondence to: Drs. Wenjing Dong and Jianjun Xiao, Department of Oncology, Zhongshan City People's Hospital, No. 2 Sunwen East Road, Zhongshan 528403, Guangdong, China. Tel: +86-0760-88823566; Fax: +86-0760-88841707; E-mail: valerie0067@163.com (WJD); xjj2215@163.com (JJX)

References

[1] Sung H, Ferlay J, Siegel RL, Laversanne M, Soerjomataram I, Jemal A and Bray F. Global cancer statistics 2020: GLOBOCAN estimates of incidence and mortality worldwide for 36 cancers in 185 countries. CA Cancer J Clin 2021; 71: 209-249.

[2] Venerito M, Link A, Rokkas T and Malfertheiner P. Review: gastric cancer-clinical aspects. Helicobacter 2019; 24 Suppl 1: e12643.

[3] Smyth EC, Nilsson M, Grabsch HI, van Grieken NC and Lordick F. Gastric cancer. Lancet 2020; 396: 635-648.

[4] Bray F, Ferlay J, Soerjomataram I, Siegel RL, Torre LA and Jemal A. Global cancer statistics 2018: GLOBOCAN estimates of incidence and mortality worldwide for 36 cancers in 185 countries. CA Cancer J Clin 2018; 68: 394-424.

[5] Torre LA, Bray F, Siegel RL, Ferlay J, Lortet-Tieulent J and Jemal A. Global cancer statistics, 2012. CA Cancer J Clin 2015; 65: 87-108.

[6] Fuse N, Kuboki Y, Kuwata T, Nishina T, Kadowaki S, Shinozaki E, Machida N, Yuki S, Ooki A, Kajiura S, Kimura T, Yamanaka T, Shitara K, Nagatsuma AK, Yoshino T, Ochiai A and Ohtsu A. Prognostic impact of HER2, EGFR, and c-MET status on overall survival of advanced gastric cancer patients. Gastric Cancer 2016; 19: 183-191.

[7] Zlotnik A and Yoshie O. The chemokine superfamily revisited. Immunity 2012; 36: 705-716.

[8] Sanchez J, Lane JR, Canals M and Stone MJ. Influence of chemokine N-terminal modification on biased agonism at the chemokine receptor CCR1. Int J Mol Sci 2019; 20: 2417.

[9] Choi JJ, Selmi C, Leung PS, Kenny TP, Roskams T and Gershwin ME. Chemokine and chemokine receptors in autoimmunity: the case of primary biliary cholangitis. Expert Rev Clin Immunol 2016; 12: 661-672.

[10] Massara M, Bonavita O, Mantovani A, Locati M and Bonecchi R. Atypical chemokine receptors in cancer: friends or foes? J Leukoc Biol 2016; 99: 927-933.

[11] Mantovani A, Bonecchi R and Locati M. Tuning inflammation and immunity by chemokine sequestration: decoys and more. Nat Rev Immunol 2006; 6: 907-918.
[12] Mollica Poeta V, Massara M, Capucetti A and Bonecchi R. Chemokines and chemokine receptors: new targets for cancer immunotherapy. Front Immunol 2019; 10: 379.
[13] Balkwill FR. The chemokine system and cancer. J Pathol 2012; 226: 148-157.
[14] Caronni N, Savino B and Bonecchi R. Myeloid cells in cancer-related inflammation. Immunobiology 2015; 220: 249-253.
[15] Massara M, Persico P, Bonavita O, Mollica Poeta V, Locati M, Simonelli M and Bonecchi R. Neutrophils in gliomas. Front Immunol 2017; 8: 1349.
[16] Lin L, Chen YS, Yao YD, Chen JQ, Chen JN, Huang SY, Zeng YJ, Yao HR, Zeng SH, Fu YS and Song EW. CCL18 from tumor-associated macrophages promotes angiogenesis in breast cancer. Oncotarget 2015; 6: 34758-34773.
[17] Keeley EC, Mehrad B and Strieter RM. CXC chemokines in cancer angiogenesis and metastases. Adv Cancer Res 2010; 106: 91-111.
[18] Liang K, Liu YR, Eer D, Liu JB, Yang F and Hu K. High CXC chemokine ligand 16 (CXCL16) expression promotes proliferation and metastasis of lung cancer via regulating the NF-κB pathway. Med Sci Monit 2018; 24: 405-411.
[19] Smith MC, Luker KE, Garbow JR, Prior JL, Jackson E, Piwnica-Worms D and Luker GD. CXCR4 regulates growth of both primary and metastatic breast cancer. Cancer Res 2004; 64: 8604-8612.
[20] Zlotnik A, Burkhardt AM and Homey B. Homeostatic chemokine receptors and organ-specific metastasis. Nat Rev Immunol 2011; 11: 597-606.
[21] Yang XL, Liu KY, Lin FJ, Shi HM and Ou ZL. CCL28 promotes breast cancer growth and metastasis through MAPK-mediated cellular anti-apoptosis and pro-metastasis. Oncol Rep 2017; 38: 1393-1401.
[22] Murakami T, Cardones AR, Finkelstein SE, Restifo NP, Klaunberg BA, Nestle FO, Castillo SS, Dennis PA and Hwang ST. Immune evasion by murine melanoma mediated through CC chemokine receptor-10. J Exp Med 2003; 198: 1337-1347.
[23] Bonavita O, Massara M and Bonecchi R. Chemokine regulation of neutrophil function in tumors. Cytokine Growth Factor Rev 2016; 30: 81-86.
[24] Sozzani S, Del Prete A, Bonecchi R and Locati M. Chemokines as effector and target molecules in vascular biology. Cardiovasc Res 2015; 107: 364-372.
[25] Kryczek I, Lange A, Mottram P, Alvarez X, Cheng P, Hogan M, Moons L, Wei S, Zou L, Machelon V, Emilie D, Terrassa M, Lackner A, Curiel TJ, Carmeliet P and Zou W. CXCL12 and vascular endothelial growth factor synergistically induce neoangiogenesis in human ovarian cancers. Cancer Res 2005; 65: 465-472.
[26] Wu YC, Tang SJ, Sun GH and Sun KH. CXCR7 mediates TGFβ1-promoted EMT and tumor-initiating features in lung cancer. Oncogene 2016; 35: 2123-2132.
[27] Uy GL, Rettig MP, Motabi IH, McFarland K, Trinkaus KM, Hladnik LM, Kulkarni S, Abboud CN, Cashen AF, Stockerl-Goldstein KE, Vij R, Westervelt P and DiPersio JF. A phase 1/2 study of chemosensitization with the CXCR4 antagonist plerixafor in relapsed or refractory acute myeloid leukemia. Blood 2012; 119: 3917-3924.
[28] Pienta KJ, Machiels JP, Schrijvers D, Alekseev B, Shkolnik M, Crabb SJ, Li S, Seetharam S, Puchalski TA, Takimoto C, Elsayed Y, Dawkins F and de Bono JS. Phase 2 study of carlumab (CNTO 888), a human monoclonal antibody against CC-chemokine ligand 2 (CCL2), in metastatic castration-resistant prostate cancer. Invest New Drugs 2013; 31: 760-768.
[29] Sandhu SK, Papadopoulos K, Fong PC, Patnaik A, Messiou C, Olmos D, Wang G, Tromp BJ, Puchalski TA, Balkwill F, Berns B, Seetharam S, de Bono JS and Tolcher AW. A first-in-human, first-in-class, phase I study of carlumab (CNTO 888), a human monoclonal antibody against CC-chemokine ligand 2 in patients with solid tumors. Cancer Chemother Pharmacol 2013; 71: 1041-1050.
[30] Fuji S, Utsunomiya A, Inoue Y, Miyagi T, Owatari S, Sawayama Y, Moriuchi Y, Choi I, Shindo T, Yoshida SI, Yamasaki S, Yamaguchi T and Fukuda T. Outcomes of patients with relapsed aggressive adult T-cell leukemia-lymphoma: clinical effectiveness of anti-CCR4 antibody and allogeneic hematopoietic stem cell transplantation. Haematologica 2018; 103: e211-e214.
[31] Ryu H, Baek SW, Moon JY, Jo IS, Kim N and Lee HJ. C-C motif chemokine receptors in gastric cancer. Mol Clin Oncol 2018; 8: 3-8.
[32] Zhou YY, Zhou B, Pache L, Chang M, Khodabakhshi AH, Tanaseichuk O, Benner C and Chanda SK. Metascape provides a biologist-oriented resource for the analysis of systems-level datasets. Nat Commun 2019; 10: 1523.
[33] Franceschini A, Szklarczyk D, Frankild S, Kuhn M, Simonovic M, Roth A, Lin J, Minguez P, Bork P, von Mering C and Jensen LJ. STRING v9.1: protein-protein interaction networks, with increased coverage and integration. Nucleic Acids Res 2013; 41: D808-815.

[34] Mantovani A, Allavena P, Sica A and Balkwill F. Cancer-related inflammation. Nature 2008; 454: 436-444.
[35] Colotta F, Allavena P, Sica A, Garlanda C and Mantovani A. Cancer-related inflammation, the seventh hallmark of cancer: links to genetic instability. Carcinogenesis 2009; 30: 1073-1081.
[36] Griffith JW, Sokol CL and Luster AD. Chemokines and chemokine receptors: positioning cells for host defense and immunity. Annu Rev Immunol 2014; 32: 659-702.
[37] Baj-Krzyworzeka M, Węglarczyk K, Baran J, Szczepanik A, Szura M and Siedlar M. Elevated level of some chemokines in plasma of gastric cancer patients. Cent Eur J Immunol 2016; 41: 358-362.
[38] Pączek S, Łukaszewicz-Zając M and Mroczko B. Chemokines-what is their role in colorectal cancer? Cancer Control 2020; 27: 1073274820903384.
[39] Chen XY, Chen RP, Jin RF and Huang ZM. The role of CXCL chemokine family in the development and progression of gastric cancer. Int J Clin Exp Pathol 2020; 13: 484-492.
[40] Shi H, Sun YX, Ruan HR, Ji C, Zhang JH, Wu PP, Li LL, Huang CH, Jia YW, Zhang X, Xu WR, Jiang JJ and Qian H. 3,3'-diindolylmethane promotes gastric cancer progression via β-TrCP-mediated NF-κB activation in gastric cancer-derived MSCs. Front Oncol 2021; 11: 603533.
[41] Coulin F, Power CA, Alouani S, Peitsch MC, Schroeder JM, Moshizuki M, Clark-Lewis I and Wells TN. Characterisation of macrophage inflammatory protein-5/human CC cytokine-2, a member of the macrophage-inflammatory-protein family of chemokines. Eur J Biochem 1997; 248: 507-515.
[42] Youn BS, Zhang SM, Lee EK, Park DH, Broxmeyer HE, Murphy PM, Locati M, Pease JE, Kim KK, Antol K and Kwon BS. Molecular cloning of leukotactin-1: a novel human beta-chemokine, a chemoattractant for neutrophils, monocytes, and lymphocytes, and a potent agonist at CC chemokine receptors 1 and 3. J Immunol 1997; 159: 5201-5205.
[43] Pardigol A, Forssmann U, Zucht HD, Loetscher P, Schulz-Knappe P, Baggiolini M, Forssmann WG and Mägert HJ. HCC-2, a human chemokine: gene structure, expression pattern, and biological activity. Proc Natl Acad Sci U S A 1998; 95: 6308-6313.
[44] Hwang JS, Kim CW, Son KN, Han KY, Lee KH, Kleinman HK, Ko J, Na DS, Kwon BS, Gho YS and Kim J. Angiogenic activity of human CC chemokine CCL15 in vitro and in vivo. FEBS Lett 2004; 570: 47-51.
[45] Yamamoto T, Kawada K, Itatani Y, Inamoto S, Okamura R, Iwamoto M, Miyamoto E, Chen-Yoshikawa TF, Hirai H, Hasegawa S, Date H, Taketo MM and Sakai Y. Loss of SMAD4 promotes lung metastasis of colorectal cancer by accumulation of CCR1+ tumor-associated neutrophils through CCL15-CCR1 axis. Clin Cancer Res 2017; 23: 833-844.
[46] Kominsky SL, Abdelmagid SM, Doucet M, Brady K and Weber KL. Macrophage inflammatory protein-1 delta: a novel osteoclast stimulating factor secreted by renal cell carcinoma bone metastasis. Cancer Res 2008; 68: 1261-1266.
[47] Weber KL, Doucet M, Shaner A, Hsu N, Huang D, Fogel J and Kominsky SL. MIP-1δ activates NFATc1 and enhances osteoclastogenesis: involvement of both PLCγ2 and NFκB signaling. PLoS One 2012; 7: e40799.
[48] Li WM, Xue WL, Wang XH, Fu XR, Sun ZC, Li ZM, Chang Y, Zhang XD, Zhou ZY, Chen CY and Zhang MZ. MiR-199a mediated the dissemination of human mantle cell lymphoma by interacting with the CCR7/CCL21 pair. Anticancer Drugs 2018; 29: 861-870.
[49] Fleige H, Bosnjak B, Permanyer M, Ristenpart J, Bubke A, Willenzon S, Sutter G, Luther SA and Förster R. Manifold roles of CCR7 and its ligands in the induction and maintenance of bronchus-associated lymphoid tissue. Cell Rep 2018; 23: 783-795.
[50] Wu S, Lu X, Zhang ZL, Lei P, Hu P, Wang M, Huang B, Xing W, Jiang XT, Liu HJ, Zhu ZG, Li WH, Zhu HF, Fu N and Shen GX. CC chemokine ligand 21 enhances the immunogenicity of the breast cancer cell line MCF-7 upon assistance of TLR2. Carcinogenesis 2011; 32: 296-304.
[51] Correale P, Rotundo MS, Botta C, Del Vecchio MT, Ginanneschi C, Licchetta A, Conca R, Apollinari S, De Luca F, Tassone P and Tagliaferri P. Tumor infiltration by T lymphocytes expressing chemokine receptor 7 (CCR7) is predictive of favorable outcome in patients with advanced colorectal carcinoma. Clin Cancer Res 2012; 18: 850-857.
[52] Chen B, Zhang D, Zhou J, Li Q, Zhou L, Li SM, Zhu L, Chou KY, Zhou L, Tao L and Lu LM. High CCR6/CCR7 expression and Foxp3+ Treg cell number are positively related to the progression of laryngeal squamous cell carcinoma. Oncol Rep 2013; 30: 1380-1390.
[53] Aggarwal S, Sharma SC and N Das S. Dynamics of regulatory T cells (T(regs)) in patients with oral squamous cell carcinoma. J Surg Oncol 2017; 116: 1103-1113.
[54] Freitas C, Desnoyer A, Meuris F, Bachelerie F, Balabanian K and Machelon V. The relevance of the chemokine receptor ACKR3/CXCR7 on CXCL12-mediated effects in cancers with a focus on virus-related cancers. Cytokine Growth Factor Rev 2014; 25: 307-316.

[55] Sun XQ, Cheng GC, Hao MG, Zheng JH, Zhou XM, Zhang J, Taichman RS, Pienta KJ and Wang JH. CXCL12/CXCR4/CXCR7 chemokine axis and cancer progression. Cancer Metastasis Rev 2010; 29: 709-722.

[56] Ieranò C, Santagata S, Napolitano M, Guardia F, Grimaldi A, Antignani E, Botti G, Consales C, Riccio A, Nanayakkara M, Barone MV, Caraglia M and Scala S. CXCR4 and CXCR7 transduce through mTOR in human renal cancer cells. Cell Death Dis 2014; 5: e1310.

[57] Wang JH, Shiozawa Y, Wang JC, Wang Y, Jung YH, Pienta KJ, Mehra R, Loberg R and Taichman RS. The role of CXCR7/RDC1 as a chemokine receptor for CXCL12/SDF-1 in prostate cancer. J Biol Chem 2008; 283: 4283-4294.

[58] Comerford I, Nibbs RJ, Litchfield W, Bunting M, Harata-Lee Y, Haylock-Jacobs S, Forrow S, Korner H and McColl SR. The atypical chemokine receptor CCX-CKR scavenges homeostatic chemokines in circulation and tissues and suppresses Th17 responses. Blood 2010; 116: 4130-4140.

[59] Park HS, Kim YM, Kim S, Lee WS, Kong SJ, Yang H, Kang B, Cheon J, Shin SJ, Kim C and Chon HJ. High endothelial venule is a surrogate biomarker for T-cell inflamed tumor microenvironment and prognosis in gastric cancer. J Immunother Cancer 2021; 9: e003353.

[60] Mizuno R, Kawada K, Itatani Y, Ogawa R, Kiyasu Y and Sakai Y. The role of tumor-associated neutrophils in colorectal cancer. Int J Mol Sci 2019; 20: 529.

[61] Wei C, Yang CG, Wang SY, Shi DD, Zhang CX, Lin XB, Liu Q, Dou RZ and Xiong B. Crosstalk between cancer cells and tumor associated macrophages is required for mesenchymal circulating tumor cell-mediated colorectal cancer metastasis. Mol Cancer 2019; 18: 64.

Table S1. Primer sequences of genes in the risk model used for qPCR

gene	primer
ACKR3	Forward: TCTGCATCTCTTCGACTACTCA
	Reverse: GTAGAGCAGGACGCTTTTGTT
CCR3	Forward: TGGCATGTGTAAGCTCCTCTC
	Reverse: CCTGTCGATTGTCAGCAGGATTA
CCL15	Forward: TCCCAGGCCCAGTTCATAAAT
	Reverse: TGCTTTGTGAGATGTAGGAGGT
CCL21	Forward: GTTGCCTCAAGTACAGCCAAA
	Reverse: AGAACAGGATAGCTGGGATGG

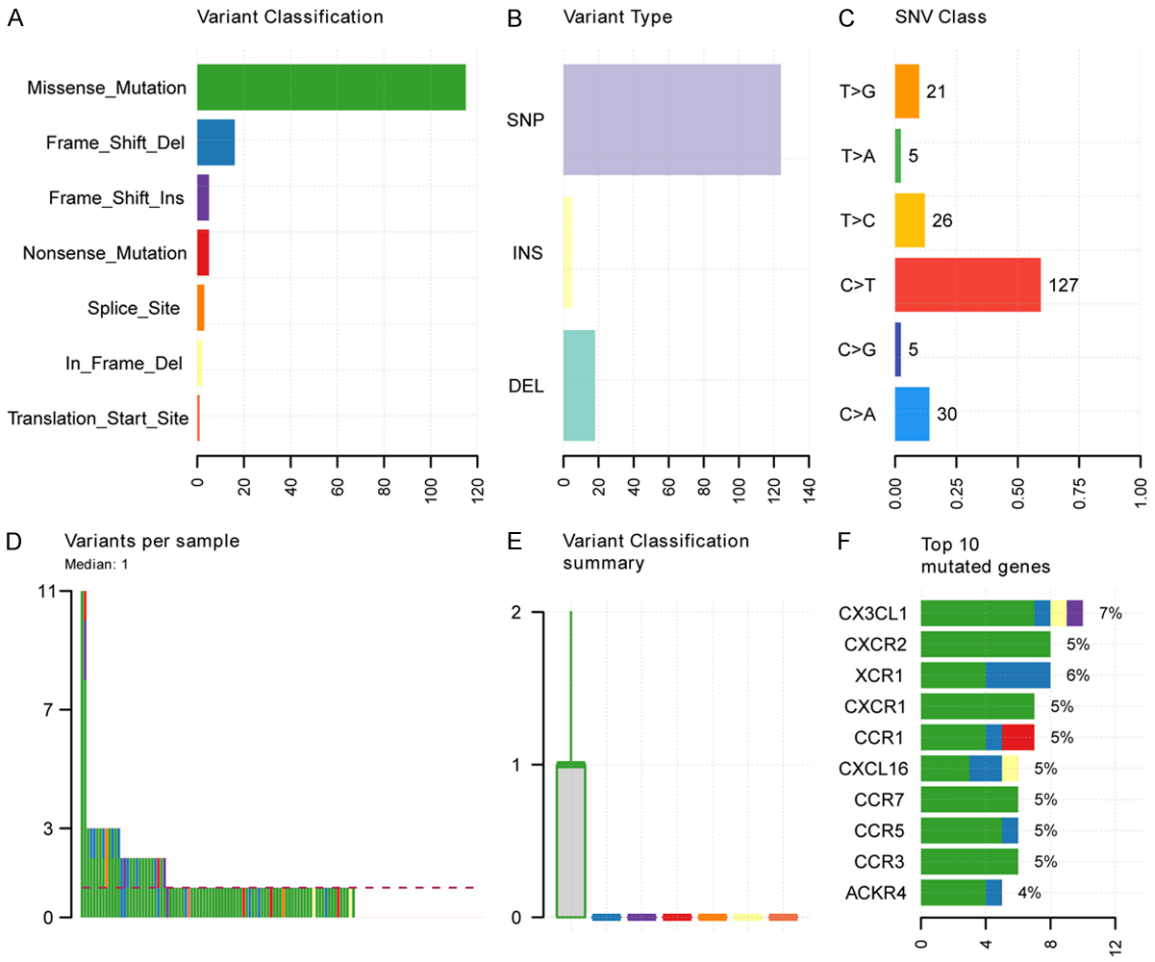

Figure S1. The overview of mutation profile of CCRs from the TCGA-STAD datasets. A. Variant classification. B. Variant type. C. SNV class. D. Variants per sample. E. Variant classification summary. F. Top 10 mutated genes.

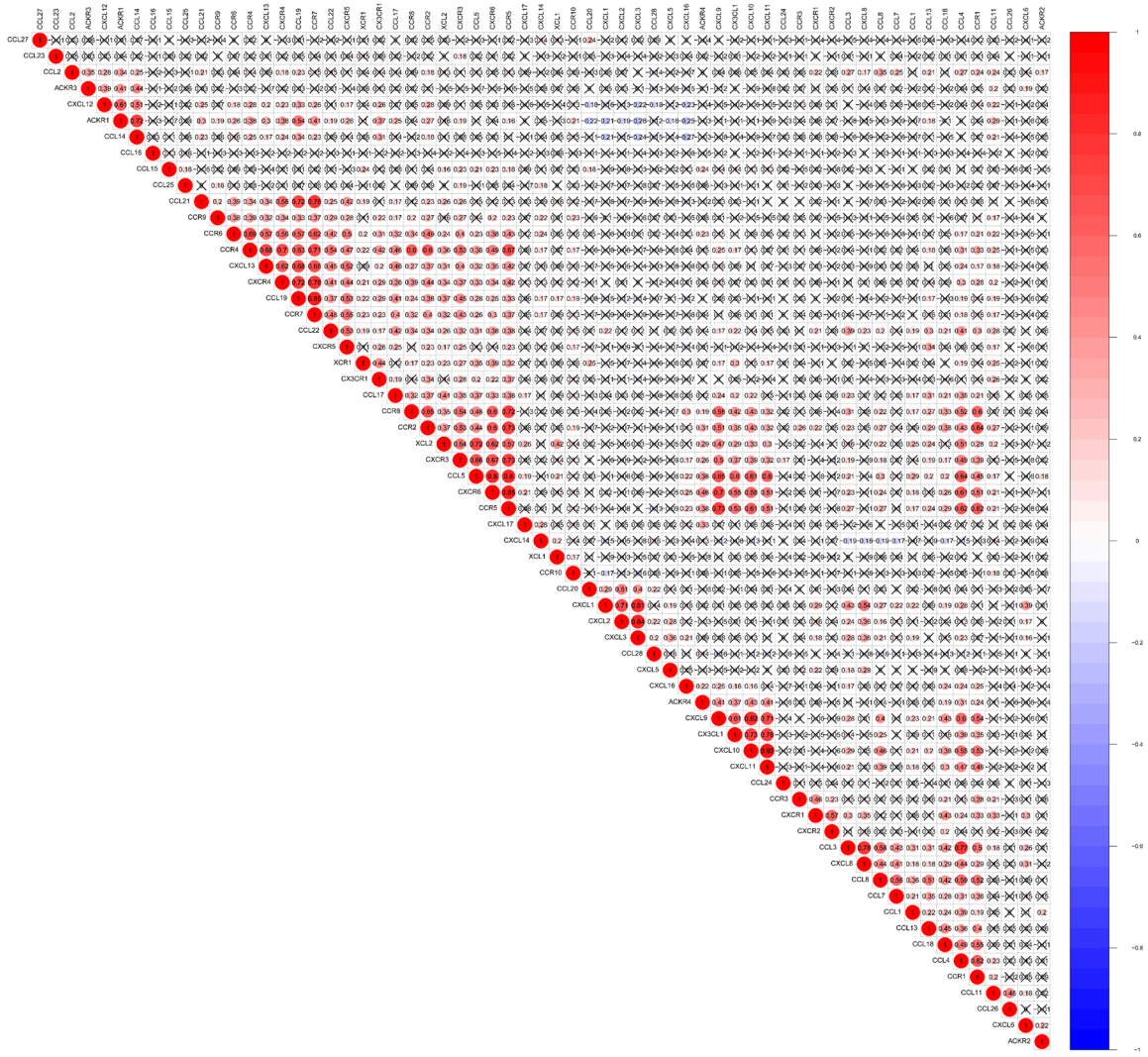

Figure S2. The correlation among CCRs. Red represents positive correlation; blue represents negative correlation. Correlation analysis was conducted by Spearman correlation analysis.

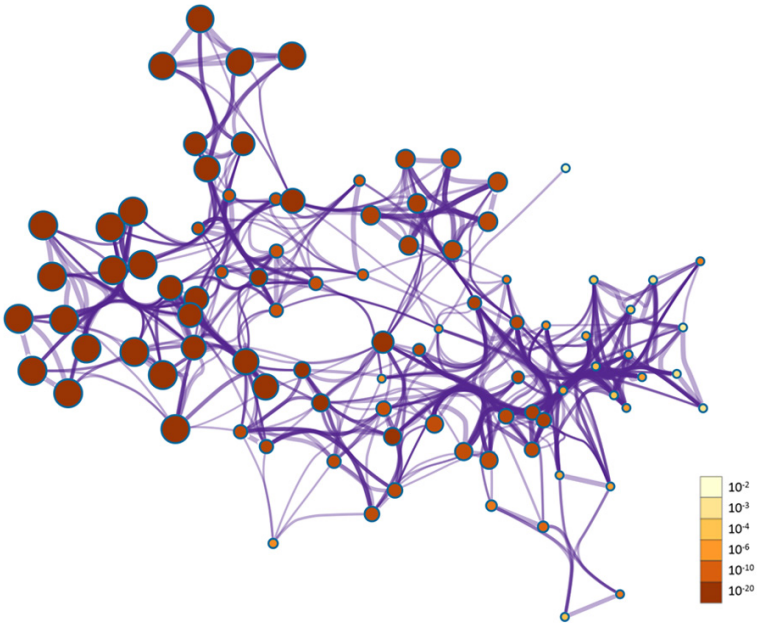

Figure S3. The *P*-value of enrichment network. The same enrichment network has its nodes colored by *P*-value (The darker the color, the more statistically significant).